Journal of Engineering Science and Technology
Vol. 20, No. 6 (2025) 1695 - 1712

THE ROLE OF ALUMINUM FOAM COATED BY GRAPHENE NANO-PAINT IN ENHANCING THE COOLING RATE IN A RADIATIVE HEAT EXCHANGER

MAMOON A. AL-JAAFARI[1], TAWFEEQ W. MOHAMMED[1,*], ALI A. SALMAN[1], MOHAMMED A. ABDULREHMAN[2]

[1]College of Engineering, Mustansiriyah University, Bab Al-Muadham, Baghdad, Iraq
[2]School of Materials and Mineral Resources Engineering, Universiti Sains Malaysia, Nibong Tebal 14300, Malaysia
*Corresponding Author: tawfeeqwasmi@uomustansiriyah.edu.iq

Abstract

An aluminium foam panel coated with graphene nano-paint is an innovative approach to enhance the heat transfer rate in a water-cooling system. For this purpose, a radiator containing aluminium foam was manufactured and used in a simple heat exchanger system. Many options have been selected to achieve optimal thermal exchange outcomes. Each time, the system utilized an aluminium foam panel with a different pore size of 1, 2, and 3 mm, which dramatically impacted the movement of the fluid and heat distribution. The system maintained the inlet water temperature at 60, 70, and 80 °C. It provides two options for water flow rates that are 1 and 3 L/min. The radiator received additional cooling from a blower that operated through forced convection near the upper part of the radiator. The tests were conducted by comparing radiators with and without the application of graphene thermal paint (GTP). The results showed that the radiator applying GTP obtained 3-5 °C better cooling outcomes than that without coating. The heat exchange enhancements resulting from GTP application, combined with increased pore sizes, lower water flow rates, and optimized aspect ratios, are fundamental elements for higher thermal effectiveness.

Keywords: Aluminum foam, Coating, Cooling, Graphene, Nano-materials.

1. Introduction

Metal foam is characterized by a solid metallic structure that includes numerous distributed pores. The pores usually occupy > 80% of the material. Metal foams are extremely interesting because of their low density and high specific strength. Aluminium foam (Al-foam) is considered a durable and lightweight material with corrosion resistance and a large surface area-to-volume ratio. Aluminium foams are either open-cell foams with interconnected pores or closed-cell foams with separated walls [1]. Aluminium foams have been used in many industrial applications, especially in operational components that require heat dissipation, such as heat exchangers and heat recovery systems, or because of their ability to withstand chemical reactions, such as using them as substrates for catalytic converters [2, 3].

Depending on the production method, the foam structure is more or less homogeneous and comprises different characteristic features that determine its properties and fields of application. Generally, manufacturers offer two basic foam structures with a range of sizes and densities. The first form is "stochastic" which has irregular-shaped pores, also known as "reticulated" It is rigid and has a highly porous and permeable structure. The second form is "regular" with stacked cells. Aluminium foams still have some restrictions in the market, and the main reason for this is the poor product quality resulting from the manufacturing processes.

However, the available manufacturing methods can control the density and other properties by manipulating the process parameters. This will facilitate the large-scale commercial acceptance of ultra-light foams for many applications. Aluminium foam production usually follows direct and indirect methods. The main methods for producing aluminium foams, also called manufacturing routes, are the melt route (liquid) [4-6] and powder metallurgical route (solid) [7, 8].

Aluminium foam is considered an auxiliary component for dissipating heat in heat exchangers and replaces the conventional methods of pipes and passages owing to the flow of fluid through porous media, which means extra surface area for heat exchange. Metal foams have been studied by several researchers for thermal applications; some of them have focused on metal-foam heat exchangers (and heat sinks), and many others have investigated the basic thermal properties of metal foams. The basic properties of metal foams include effective thermal conductivity, density, and permeability. The shape, structure, and features of the foam strongly influence the thermal characteristics of Al-foams [9].

Aluminium foam and its corresponding thermal applications, especially those related to heating or cooling, have attracted significant attention from researchers owing to their sufficient heat exchange, simplicity, use for both liquid and gas flow, and economic impact [10]. In this perspective, several studies have used Al-foam for heating. For example, a source of heat generation, usually an electrical heater or, in some cases, a hot water coil, can be attached to a rectangular foamed panel, where water (or ethylene glycol) flows across the foam and gets heated [11, 12]. The foam can be inserted into the stream in a way that allows it to be easily removed and renovated several times [13] or as a separate element in the system [14].

Steam can also be used to heat water, where metallic foam can be inserted inside a water flow tube as several discontinuous cylindrical pieces with limited length [15]. Air can be heated by passing it across the foamed section [16, 17] or recirculating it inside

the metallic foam heat exchanger [18, 19]. Aluminium foam cylinders can also be fabricated with bundles of hot fluids to heat air under cross-flow [20].

In contrast, several studies have presented metallic foams for cooling purposes. For example, foam has been used as an alternative to fins in water-to-air heat exchangers [21] or as an effective method for air-cooling heat exchangers [22, 23]. In one study, metallic foam was exposed to very hot gases, and the coolant was cold air [24]. In addition, metal foam has been used for electronic cooling applications by implementing the foam in a fined box to remove heat from the hot surface of an appliance to the air [25, 26] or to reduce the battery temperature [27]. Some studies have focused on the simulation of the cellular structures of general metallic foams and their relation to heat exchanger parameters [28].

Furthermore, a composite of metal foam and phase change material has shown a shorter melting process, thus resulting in a higher heat transfer rate in a triplex-tube heat exchanger [29]. Previous studies have advised the use of open-cell Al-foams with a density of less than 1 g/cm^3 and pore size between 0.5-4 mm. High porosity is preferred (more than 80%), although some studies have reported lower porosities. The port density is usually between 10-100 PPI, but it is preferable to be higher than 40 PPI to ensure high volumetric flow. The shapes and dimensions of the foamed panels may differ from one system to another, depending on the application required.

Nanotechnology can be implemented in Al-foam for cooling purposes by using highly thermally conductive nanomaterials, such as graphene. Graphene is a graphite layer with a hexagonal lattice of carbon atoms bonded in an atomic group. Graphene nanoparticles (GNPs) have become a matter of interest in the recent years as a reinforcement material in many composites due to the remarkable enhancement in the properties of based materials. The mechanical properties can be enhanced by increasing the interphase contact and reducing the surface antiparticle distance, which may enhance the strength and toughness. Furthermore, graphene has shown superior thermal conductivity, thus it can be used in applications related to heating and cooling [30, 31].

Coating or painting metal with graphene is an interesting method to take advantage of the high thermal conductivity of graphene to enhance the heat transfer rate. Paints containing carbon-based nanomaterials enhance the thermal conductivity and confer greater heat dissipation to the surface. Carbon-based nanomaterials increase the thermal conductivity of paint by more than 100% and increase heat transmission. When used on metal surfaces, the efficiency of heat dissipation increases, which is extremely useful in applications requiring cooling [32, 33].

Many studies have sought to use graphene to enhance the characteristics of metallic foams for many applications by improving their physical and chemical features [34], enhancing their mechanical properties [35, 36], or specifically enhancing the effective thermal conductivity of the metallic foam [37, 38].

However, the literature shows a lack of interest in investigating the role of adding graphene as paint to metallic foam for cooling purposes. The use of graphene-based nanomaterials as a coating layer can be useful to enhance the cooling efficiency owing to the extremely high thermal conductivity of graphene (up to 4000 W/(m·K) [39]). This accelerated the cooling rate. The aim was to evaluate the thermal performance resulting from the improvement in the thermal

conductivity of the painted surfaces of the panels. In the current study, an aluminium foam panel coated with graphene was used as a radiator component in a heat-exchanging system for water cooling. This study seeks to determine the improvement in cooling efficiency due to the coating and compare it with the case of an uncoated Al-foam panel.

2. Materials and Methods

2.1. The materials used

The radiator under consideration consists of a metallic case that contains an aluminium foam panel coated with graphene nano-paint. The materials were purchased from the local market. The foamed aluminium panels were manufactured by a Chinese company (Guangzhou Sailong). Three panels with different pore sizes (1, 2, and 3 mm) were selected. Each one had dimensions of 30 × 20 × 5 cm^3. The graphene nanopowder was manufactured by a Chinese company (XFNANO). Urea-formaldehyde glue was used as a resin for the nano-paint. The characteristics of the materials used are listed in Table 1.

Table 1. Properties of the materials used in the study*.

Material	Specifications
Al-foam	The porosity of the panel is ranged between 70-80% and the density is ranged between 0.8-1 g/cm^3.
Graphene	High purity black powder (diameter < 30 nm), apparent density of 0.06 g/cm^3, low oxygen and easy to disperse in solvents.
Urea-formaldehyde	Transparent liquid, viscosity of 450 mPa.s at 20 ^oC and density of 1.40 g/cm^3.

***As appeared on the data sheet of the product (Guangzhou Sailong).**

The paint was prepared by carefully mixing the nanopowder into the resin. Initially, the desired quantity of resin was heated to 70 °C using an electrical heater to reduce the matrix viscosity and facilitate the dispersion of the particles. A precise quantity of the nano-powder was then dispersed into the resin using bath ultra-sonication. The powder was poured at a concentration of 20%, followed by mixing the solution in a suitable container using a high-speed stirrer at 1000 rpm for half an hour. This procedure satisfies the homogeneous dispersion of nanomaterials in the matrix. The solution was then cooled to room temperature. However, high temperatures accelerate the curing rate, causing disorder chains. However, cool temperatures slow the curing rate, which means a longer time for the product to heal completely [40].

Finally, the solution was weighed again to ensure the required total mass. The solution was then poured into the tank of the coating machine and sprayed onto the required surfaces. The paint should be applied to dry surfaces. The average coating thickness was 1.2-1.5 mm, as measured using an ultrasonic thickness gauge. The initial curing time is 4 h, but it takes 7 days for full curing. The paint has chemical resistance, hydrophobic properties, and durability for 1 year [41]. Figure 1 shows the materials used in this study. The coating process is illustrated in Fig. 2.

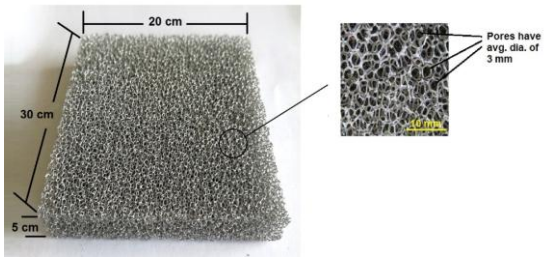

(a) Aluminum foam.

(b) Graphene nano-powder (Avg. dia.<30 nm).

Fig. 1. Material used in the current study.

(a) Mixing the powder with resin and ultra-sonication.

(b) Spraying the paint.

(c) Measuring the thickness of the coating.

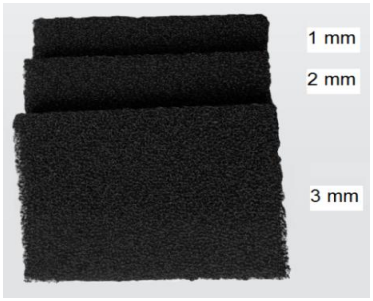

(d) Samples ready for using with different pore diameters.

Fig. 2. Processes of coating the aluminium panels by graphene nano-paint.

2.2. The utilized rig

Experimental work has been conducted to evaluate the thermal efficiency of a radiator made of aluminium foam and coated with graphene for water cooling. The study was conducted experimentally in the Workshop Lab at the College of Engineering, Mustansiriyah University (Iraq) during the period 3-24 April 2024. Al-foam panel has been served as a radiator for heat dissipation purpose in a cooling system with two configurations: firstly, without graphene thermal paint and then with graphene thermal paint.

The system is an open cycle water flow mechanism that contains an upper tank, lower tank, Al-foam radiator, connectors, heater, air blower, flow meter, and thermometer. An electrical heater was used to heat the water. An air blower was used to cool the radiator via forced convection using indoor air. The operation begins by heating the water to a certain high temperature (60-80 °C), which remains constant during each test. The water flows downward toward the radiator by gravity.

The panel was placed in a metallic box and sealed well in order to control the water flow passing through the lower portion and the airflow across the upper portion. Thus, water enters the panel from one side, passes through the cellular structure, and leaves from the other side. The collected water then flowed to the lower tank, as shown in Fig. 3. Note that the air has a semi-cross flow because it passes over the upper half of the foam depending on the aspect ratio. where the aspect ratio is the water altitude in the container to the total radiator height.

The discharge of water in the cycle was measured using a flow meter. A thermometer was used to measure the temperatures at many locations within the system. The measurements in each test continued until a steady-state temperature was obtained, which took approximately 2 min depending on the flow characteristics. The specifications of these components are listed in Table 2.

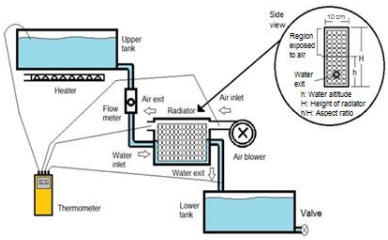

(a) Schematic draw of the system.

(b) Actual view of the rig.

Fig. 3. Schematic diagram of the system.

Table 2. Specifications of system components.

Component	Specifications
Upper tank	Capacity is 60 L (not filled).
Lower tank	Capacity is 40 L (not filled).
Radiator	Metallic box of 40 × 30 × 10 cm^3 has Al-foam of 30 × 20 × 5 cm^3 inside with passages for water and air.
Connectors	Plastic tubes of ½ inch diameter.
Heater	Electrical device of 4000 W.
Air blower	Electrical device of 1000 W, 2.3 m^3/min capacity and 2 inch exit diameter.

2.3. The instruments

The main tools used for the measurements were a flow meter and thermometer. The specifications of the instruments used are presented in Table 3. A flow meter was used to measure the discharge of water entering the radiator. A thermometer data logger was used to measure the temperature at four locations: inlet water to the radiator (the thermocouple was submerged in the upper tank), exit water from the radiator (the thermocouple was attached to the water flow just before entering the lower tank), inlet air (the thermocouple was attached to the air flow just before entering the radiator), and exit air (the thermocouple was attached to the air flow just after leaving the radiator). The thermocouples used were of type (K).

Table 3. Specifications of instruments.

Item.	Features
Thermometer	Type (Reed SD-947), 4 ports (error is less than ±0.5 °C).
Flow meter	Type (Flowtech), up to 6 LPM flow rate (less than 4% error).

2.4. The operational conditions

In the current study, the operational conditions, limitations, and ranges of the measured parameters are listed in Table 4.

Table 4. Operational conditions.

Item.	Features
Water temperature at radiator inlet	60, 70 and 80 °C
Water flow rate at radiator inlet	1 and 3 LPM
Air temperature at radiator inlet	25 °C
Aspect ratio (h/H)	0.3, 0.6 and 0.9
Al-foam pore size	1, 2 and 3 mm
Feature of Al-foam panel	With and without GTP

As a result, the experimental works included several case studies, as shown in Fig. 4.

3. Results and Discussion

The study includes several measurements of the model built for the proposed cooling system using an Al-foam radiator as a heat exchanger. The system was compared for two main configurations of Al-foams: with and without graphene thermal paint (GTP).

The general results showed a decrease in the outlet temperature from the radiator owing to the use of GTP. The results showed that the suggested system requires no less than 2 min of circulation to ensure a reliable decrease in the hot water temperature passing through the Al-foam radiator. In this case, the

temperature at the exit will be lower than that at the entrance by several degrees, depending on the conditions.

By examining individual cases, Fig. 5 shows the results for the case of a pore size of 1 mm with a flow rate of 1 LPM. The exit temperature was initially close to the inlet temperature, but after 60 s, it reduced faster and then settled to a steady-state temperature. However, the time required for the water level to decrease and settle was higher when using a higher flow rate of 3 LPM, as shown in Fig. 6. By using Al foam with a higher pore size, the cooling was faster, as shown in Fig. 7.

However, the cooling rate decreased again when a higher flow rate was used, as shown in Fig. 8. When a larger pore size (3 mm) was used, the cooling was faster, usually after 40 s, as shown in Fig. 9. However, it slowed down again when a flow rate of 3 LPM was used, as shown in Fig. 10. The results of using different aspect ratios are also presented in Figs. 11 and 12 for aspect ratios of 0.3 and 0.9, respectively. The last two cases showed a longer time to reach the steady state than the case that used an aspect ratio of 0.6.

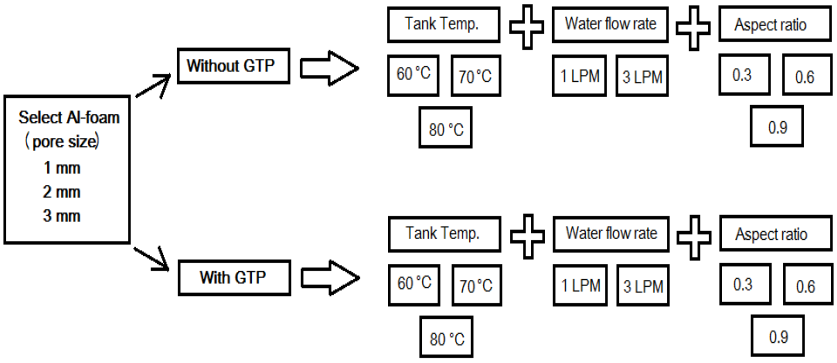

Fig. 4. Flow chart shows the case studies.

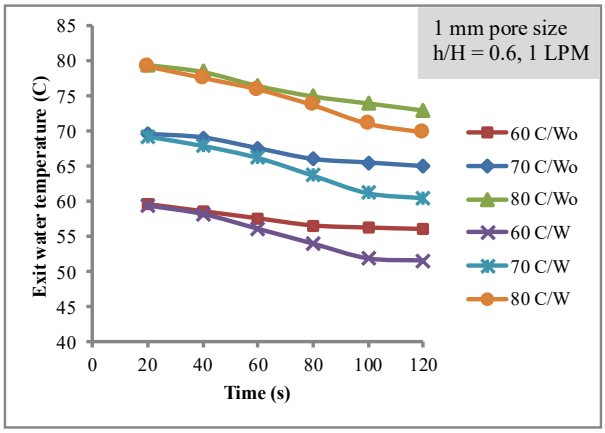

Fig. 5. Reduction in hot water temperature passing through Al-foam of 1 mm pore size with (W) and without (Wo) graphene thermal paint (1 LPM discharge & 0.6 aspect ratio).

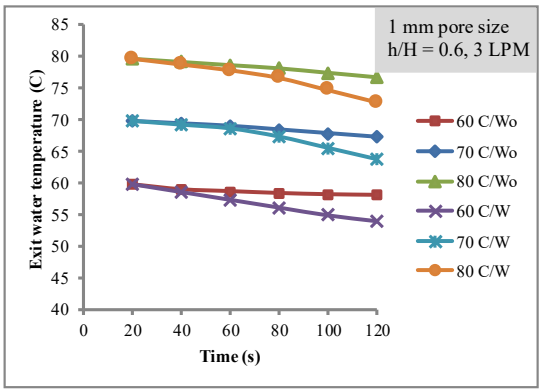

Fig. 6. Reduction in hot water temperature passing through Al-foam of 1 mm pore size with (W) and without (Wo) graphene thermal paint (3 LPM discharge & 0.6 aspect ratio).

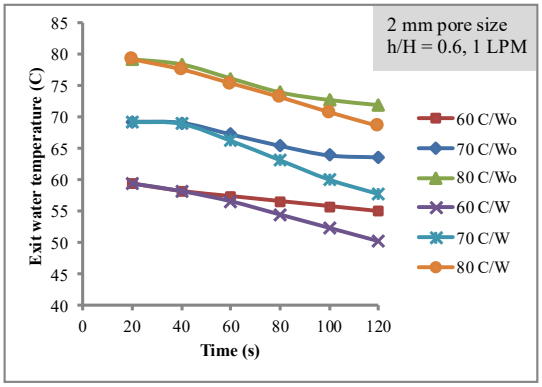

Fig. 7. Reduction in hot water temperature passing through Al-foam of 2 mm pore size with (W) and without (Wo) graphene thermal paint (1 LPM discharge & 0.6 aspect ratio).

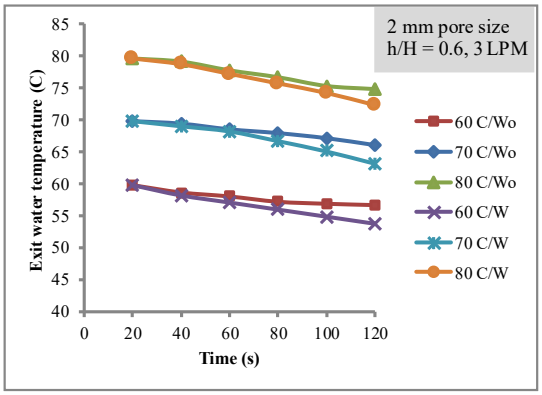

Fig. 8. Reduction in hot water temperature passing through Al-foam of 2 mm pore size with (W) and without (Wo) graphene thermal paint (3 LPM discharge & 0.6 aspect ratio).

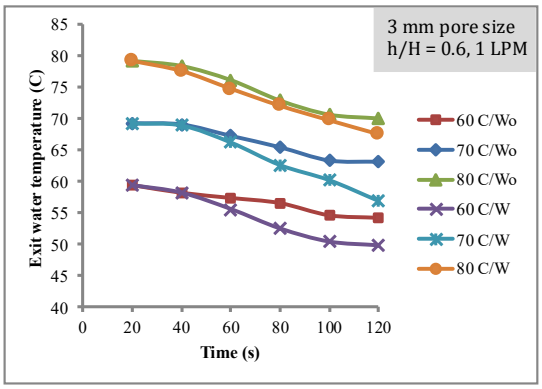

Fig. 9. Reduction in hot water temperature passing through Al-foam of 3 mm pore size with (W) and without (Wo) graphene thermal paint (1 LPM discharge & 0.6 aspect ratio).

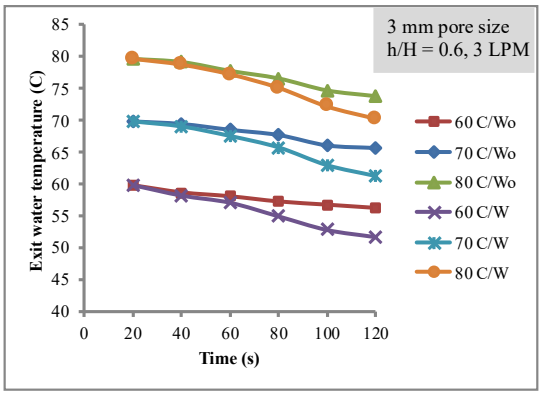

Fig. 10. Reduction in hot water temperature passing through Al-foam of 3 mm pore size with (W) and without (Wo) graphene thermal paint (3 LPM discharge & 0.6 aspect ratio).

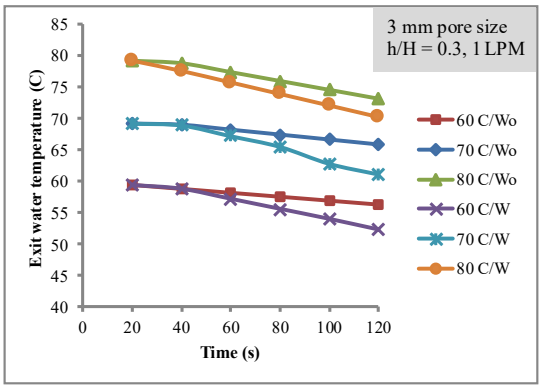

Fig. 11. Reduction in hot water temperature passing through Al-foam of 3 mm pore size with (W) and without (Wo) graphene thermal paint (1 LPM discharge & 0.3 aspect ratio).

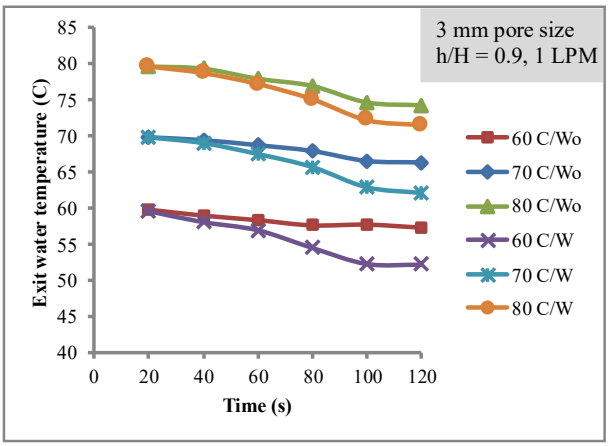

Fig. 12. Reduction in hot water temperature passing through Al-foam of 3 mm pore size with (W) and without (Wo) graphene thermal paint (1 LPM discharge & 0.9 aspect ratio).

To ensure sufficient cooling, heat was initially transferred from the hot water in the radiator container to the rigid aluminium structure and the cell pores within. The presence of pores in the foam plays a major role in the heat capacitance owing to the additional contact surface area provided by the pores. The heat was transferred quickly from the lower part of the panel to the upper part owing to the potential action of the forced air supplied by the fan.

The exit temperature is lower than that measured at the inlet by 4-12 °C in general. The effect of coating the aluminium panel with graphene was interesting, where the cooling capacity of Al-foam with GTP was higher than that of Al-foam without GTP. The cooling capacity for the case with GTP was 3-5 °C better than that without GTP. This is due to the contribution of graphene as a superthermally conductive nanomaterial.

One of the other notices is the impact of inlet water temperature. The warmest inlet water (80 °C) exhibited a higher cooling capacity (by 7-12 °C) than the less warm water (60 °C), which was lower by 2-5 °C. This is attributed to several factors, such as the structure of the warmer water during cooling and convection currents that produce different non-uniform temperature distributions [42].

In the case of using a higher flow rate (3 LPM) instead of a lower one, the heat capacity was lower. This is due to the impact of circulation. Where a continuous re-mixing process with a corresponding energy balance occurs in the container; and the water in the container is cooled to a temperature lower than that entered. However, at higher flow rates, the time for mixing and the time for releasing will not be sufficient to ensure appropriate heat exchange. This phenomenon has also been mentioned by some researchers [43], where slow flow rates in circulating media expose higher heat exchange. Therefore, a larger quantity of water implies more heat to be stored in the water. This explains why the cooling rate was lower when the water discharge was 3 LPM rather than 1 LPM.

The structure of the Al foam has another effect. It was observed that the cooling rate was higher when the pore size was 3 mm than at lower pore sizes (1 and 2

mm). This is due to the larger internal surface area of the 3 mm pore cell that is exposed to hot water in the container, thus playing a significant role in dissipating a higher amount of heat. However, Zhang et al. [44] examined the effect of pore size on the heat transfer performance of porous copper, where samples with medium pore sizes exhibited better heat transfer coefficients than samples with smaller or larger pore sizes. They explained that small pores result in a greater flow resistance. Conversely, larger pores lead to longer flow paths.

A subsidiary investigation, focused on the role of aspect ratio (water altitude in the container to the whole radiator height), showed that the decrease in this ratio from 0.6 to 0.3 was not useful owing to the limitation of water quantity within the container to play an effective role in the cooling, where a massive amount of hot water just passed to the other side without sufficient cooling (high bypass ratio). However, increasing this ratio from 0.6 to 0.9 was not useful because of the reduction in the surface area of the Al-foam part exposed to air, resulting in less convection heat transfer.

The effectiveness (ϵ) of a heat exchanger is defined as the ratio of the actual heat transfer to the maximum possible heat transfer [45]. Hence, the effectiveness of the radiator can be expressed as:

$$\epsilon = \frac{T_{hi} - T_{ho}}{T_{hi} - T_{ci}} \quad (1)$$

where, T_{hi} is inlet water temperature, T_{ho} is exit water temperature, T_{ci} is inlet air temperature.

The water temperatures at the exit point for each case are listed in Table 5. It can be seen clearly that the case of Al-foam with a 3 mm pore size (1 LPM discharge and 0.6 aspect ratio) showed the optimum reduction. The cooling capacity is ranged between 4-9 °C in general for the foam without GTP. However, it ranged between 5-12 °C for the case with GTP.

Table 5. Values of outlet water temperature for different cases.

It.	Case study	T_{ho} without GTP			T_{ho} with GTP		
	Inlet water temperature (°C)	**60**	**70**	**80**	**60**	**70**	**80**
1	Al-foam of 1 mm pore size (1 LPM discharge & 0.6 aspect ratio)	56.1	65.1	73.0	51.5	60.5	69.9
2	Al-foam of 1 mm pore size (3 LPM discharge & 0.6 aspect ratio)	58.0	67.2	76.7	54.1	63.7	72.8
3	Al-foam of 2 mm pore size (1 LPM discharge & 0.6 aspect ratio)	54.9	63.6	71.9	50.2	57.7	68.5
4	Al-foam of 2 mm pore size (3 LPM discharge & 0.6 aspect ratio)	56.7	66.0	74.7	53.7	63.2	72.3
5	Al-foam of 3 mm pore size (1 LPM discharge & 0.6 aspect ratio)	54.2	63.1	70.1	49.7	56.9	67.5
6	Al-foam of 3 mm pore size (3 LPM discharge & 0.6 aspect ratio)	56.2	65.7	73.7	51.7	61.2	70.3
7	Al-foam of 3 mm pore size (1 LPM discharge & 0.3 aspect ratio)	56.3	65.8	73.1	52.2	61.1	70.3
8	Al-foam of 3 mm pore size (1 LPM discharge & 0.9 aspect ratio)	57.3	66.3	74.2	52.2	62.1	71.5

The effectiveness results (average values at 60, 70, and 80 °C) for all the case studies are listed in Table 6. General notices declare the enhancement in the heat exchanger effectiveness due to the use of the following factors: GTP, larger pore size, lower water discharge, and an aspect ratio of 0.6. However, the results showed that the best configuration was the Al-foam with a 3 mm pore size (1 LPM discharge & 0.6 aspect ratio) with GTP, where the average effectiveness was 27%. The lowest effectiveness was 6% using Al-foam with a 1 mm pore size (3 LPM discharge & 0.6 aspect ratio) without GTP. Although the effectiveness values in this study were lower than the common values at high air velocities (usually more than 40% [46]), the study has encouraged data to involve graphene-based materials in improving the thermal performance of Al-foam panels in the cooling process.

Table 6. Average values of effectiveness for different cases.

Item	Case study	Effectiveness without GTP (%)	Effectiveness with GTP (%)
1	Al-foam of 1 mm pore size (1 LPM discharge & 0.6 aspect ratio)	11.6	21.3
2	Al-foam of 1 mm pore size (3 LPM discharge & 0.6 aspect ratio)	6.0	14.4
3	Al-foam of 2 mm pore size (1 LPM discharge & 0.6 aspect ratio)	14.4	25.4
4	Al-foam of 2 mm pore size (3 LPM discharge & 0.6 aspect ratio)	9.3	15.7
5	Al-foam of 3 mm pore size (1 LPM discharge & 0.6 aspect ratio)	16.6	27.1
6	Al-foam of 3 mm pore size (3 LPM discharge & 0.6 aspect ratio)	10.7	20.3
7	Al-foam of 3 mm pore size (1 LPM discharge & 0.3 aspect ratio)	10.5	19.9
8	Al-foam of 3 mm pore size (1 LPM discharge & 0.9 aspect ratio)	8.8	18.5

A brief comparison of the current findings with those of other studies on nano-painting is presented in Table 7. The works satisfy an average cooling capacity between 2-8 ˚C. The thermal performance and effectiveness were enhanced by 10-15%.

Table 7. Comparison for the findings of different research.

Ref.	Description of the work	Main findings
Current work	This study investigates the role of nano-coated metallic foam in enhancing the cooling rate in a radiative heat exchanger	There is an increase in the cooling capacity by 2-3 °C more for the case with graphene paint. The effectiveness is enhanced to 29% with the graphene paint (15% increasing).
Pongiannan et al. [47]	Nano-coating was employed in an aluminum heat sink to study the heat transfer performance.	The surface temperature decreased between 2-5 °C.
Sabarish et al. [48]	Nano-graphene coating applied on metallic extended surfaces for heat exchange.	Heat transfer has been enhanced by 10%. The surface temperature decreased between 5-8 °C.
Hasan et al. [49]	General review paper.	Nano-coating may lead to 10% increase in thermal capacity.

However, to increase the effectiveness of the cooling, it is suggested to mix the graphene nanomaterials within the aluminium structure during the formation of the foam. This configuration helps to gain the benefits of heat exchange with the cellar foam as well as the graphene that is incorporated close to the interfacial layer up to the core; hence, it increases heat transfer in all directions.

The measured quantities exhibited some deviations compared to the calculated values owing to errors in the instruments. These individual uncertainties were presented in a simple analysis suggested by Kline and McClintock [50] to determine the overall uncertainty error. The overall uncertainty error (e_R) is given by:

$$e_R = \left[\left(\frac{\partial R1}{\partial Xn} e_{X1}\right)^2 + \left(\frac{\partial R2}{\partial Xn} e_{X2}\right)^2 + \cdots + \left(\frac{\partial R3}{\partial Xn} e_{Xn}\right)^2\right]^{1/2} \quad (2)$$

In the current study, the effective measured values are the water flow rate ($\dot{m}$) and water temperature (T); therefore, the governorate equation that involves these parameters is,

$$Q = \dot{m}\, C_p\, (Tw - T) \quad (3)$$

Now the derivatives with respect to the variables are:

$$\frac{\partial Q}{\partial \dot{m}} = C_p\, (Tw - T) \quad (4)$$

$$\frac{\partial Q}{\partial T} = -\dot{m}\, C_p\, Tw \quad (5)$$

Now, the data recorded for certain conditions at the steady-state are:

1 LPM, Tw=60 ºC, T=51.5 ºC (for 1 mm pores with GTP)

The individual errors for each effective parameter are:

e1 = 0.04 (for flow meter)

e2 = 0.005 (for thermometer)

By substituting the recorded values for a certain case, the error value did not exceed 2%.

4. Conclusions

This study investigated the role of nano-coated metallic foam in enhancing the cooling rate of a radiative heat exchanger. The work was performed experimentally by coating the aluminium foam with graphene nanocolor in a certain method and then testing it on a rig. The thermal performance of the foam was analysed based on the amount of cooling effect. The following are the conclusions drawn from this study:

- There is a noticeable enhancement in the heat exchanger effectiveness due to the use of GTP with aluminium foam.
- Factors that increase the thermal performance are a larger pore size, lower water discharge, and an aspect ratio of 0.6.
- The cooling capacity was generally in the range of 4-9 °C in general for the foam without GTP, whereas it was ranged of 5-12 °C for the case with GTP.

- The effectiveness was enhanced in certain cases from 6% without GTP to 29% with GTP.

References

1. Patel, N.; Mittal, G.; Agrawal, M; and Pradhan, A.K. (2024). Aluminum foam production, properties, and applications: A review. *International Journal of Metalcasting*, 18(3), 2181-2198.
2. Garai, F. (2020). Modern applications of Aluminium foams. *International Journal of Engineering and Management Sciences* (*IJEMS*), 5(2), 14-21.
3. Hommel, P.; Roth, D.; and Binz, H. (2021). Derivation of motivators for the use of aluminum foam sandwich and advantageous applications. *Proceedings of the Design Society*, 1, 933-942.
4. Wang, L.; Wang, Y.; You, X.; and Wang, F. (2020). Foaming behavior and pore structure evolution of foamed aluminum under the extrusion constraint. *Advances in Materials Science and Engineering*, 2020(1), 3948378.
5. Rathore, S.; Singh, R.K.R.; and Khan, K.L.A. (2021). Effect of process parameters on mechanical properties of aluminum composite foam developed by friction stir processing. *Proceedings of the Institution of Mechanical Engineers*, *Part B*: *Journal of Engineering Manufacture*, 235(12), 1892-1903.
6. Sangeetha, M.; Prakash, S.; Sridharraja, K.S.; and Muralimano, J. (2022). Development, testing and microstructural study of aluminum foam in automobile application. *International Journal of Ambient Energy*, 43(1), 2568-2576.
7. Mohammed, S.H.; and Aljubouri, A.A. (2016). Manufacturing of aluminum foam as a light weight structural material. *Eng. &Tech. Journal*, 34(5), 697-702.
8. Papantoniou, I.G.; Pantelis, D.I.; and Manolakos, D.E. (2018). Powder metallurgy route Aluminium foams: A study of the effect of powder morphology, compaction pressure and foaming temperature on the porous structure. *Procedia Structural Integrity*, 10, 243-248.
9. Rajak, D.K.; and Gupta, M. (2020). *An Insight into Metal Based Foams*: *Processing*, *Properties and Applications*. Springer.
10. Han, X.-H.; Wang, Q.; Park, Y.G.; T'Joen, C.; Sommers A.; and Jacobi, A. (2012). A review of metal foam and metal matrix composites for heat exchangers and heat sinks. *Heat Transfer Engineering*, 33(12), 991-1009.
11. Boomsma, K.; Poulikakos, D.; and Zwick, F. (2003). Metal foams as compact high performance heat exchangers. *Mechanics of Materials*, 35(12), 1161-1176.
12. Fernandez-Morales, P.; Nieto, C.; Patiño, C.; Lopez, J.P.; Tamayo, D.; Mendoza, E.; and Giraldo, M. (2014). A conceptual design of energy exchange system for recovery of residual heat using aluminum foams. *Procedia Materials Science*, 4, 371-376.
13. Prabha, S. (2018). Manufacture and evaluation of cast aluminum foam heat exchangers. Retrieved December 12, 2023, from https://etd.iisc.ac.in/handle/2005/3974.
14. Ozmat, B. (2018). Metal foam heat exchangers. Retrieved December 12, 2023, from https://www.electronics-cooling.com/2018/06/metal-foam-heat-exchangers/

15. Abdul-Sahib, A.A.; and Muneer, A. (2021). Experimental steam condensation enhancement on metal foam filled heat exchanger. *Journal of Mechanical Engineering Research and Developments*, 44(4), 145-167.
16. Bhaskar, B.S.; and Choudhary, S.K. (2017). Experimental investigation of heat transfer through porous material heat exchanger. *International Journal of Engineering Research and Technology*, 10(1), 51-60.
17. Donmus, S.; Mobedi, M.; and Kuwahara, F. (2021). Double-layer metal foams for further heat transfer enhancement in a channel: An analytical study. *Energies*, 14(3), 672.
18. Buonomo, B.; Di Pasqua, A.; Ercole, D.; and Manca, O. (2019). The effect of PPI on thermal parameters in compact heat exchangers with aluminum foam. *Journal of Physics*: *Conference Series*, 1224(1), 012045.
19. Sun, K.; Zhou, G.-Y.; Luo, X.; Tu, S.-T.; and Huang, Y.-Y. (2022). Study on enhanced heat transfer performance of open-cell metal foams based on a hexahedron model. *Numerical Heat Transfer*, *Part A*: *Applications*, 82(7), 335-355.
20. Chumpia, A.; and Hooman, K. (2019). Performance of tubular aluminum foam heat exchangers in multiple row bundles. *Journal of Thermal Analysis and Calorimetry*, 135(3), 1813-1822.
21. Dongellini, M.; Naldi, C.; Cancellara, S.; and Morini, G.L. (2022). Experimental measurements of thermal-hydraulic performance of aluminum-foam water-to-air heat exchangers for a HVAC application. *Applied Thermal Engineering*, 213, 118716.
22. Dai, Z.; Nawaz, K.; Park, Y.; Chen, Q.; and Jacobi, A. (2012). A comparison of metal-foam heat exchangers to compact multilouver designs for air-side heat transfer applications. *Heat Transfer Engineering*, 33(1), 21-30.
23. Nawaz, K.; Bock, J.; and Jacobi, A.M. (2017). Thermal-hydraulic performance of metal foam heat exchangers under dry operating conditions. *Applied Thermal Engineering*, 119, 222-232.
24. Hafeez, P.; Esmaeelpanah, J.; Chandra, S.; and Mostaghimi, J. (2013). Heat transfer through metal-foam heat exchanger at higher temperature. *Proceedings of the ASME* 2013 *Heat Transfer Summer Conference collocated with the ASME* 2013 7th *International Conference on Energy Sustainability and the ASME* 2013 11th *International Conference on Fuel Cell Science, Engineering and Technology*, Minneapolis, Minnesota, USA, 1-5.
25. Ataer, S.K.; Yamali, C.; and Albayrak, K. (2020). A comparison of the thermal performance of a conventional fin block and partially copper and aluminum foam embedded heat sinks. *J. of Thermal Science and Technology*, 40(1), 155-165.
26. Glass, J. (2021). *Modelling and optimization of metal foam integrated heat exchangers for power electronics cooling*. PhD Thesis, Department of Mechanical engineering, Université Grenoble Alpes.
27. Wang, P.; Qin, D.; Wang, T.; and Chen, J. (2022). Thermal performance analysis of gradient porosity aluminium foam heat sink for air-cooling battery thermal management system. *Applied Sciences*, 12(9), 4628.
28. Chin, A.R.; Kurnia, J.C.; and Sasmito, A.P. (2022). Pore-scale modeling in metal foam heat exchanger. *ECS Transactions*, 107(1), 7713-7722.

29. NematpourKeshteli, A., Iasiello, M., Langella, G., and Bianco, N. (2022). Enhancing PCMs thermal conductivity: A comparison among porous metal foams, nanoparticles and finned surfaces in triplex tube heat exchangers. *Applied Thermal Engineering*, 212, 118623.
30. Hareesha, M.; Yogesha, B.; Naik, L.L.; and Saravanabavan. D. (2021). Development on graphene based polymer composite materials and their applications-A recent review. *Proceedings of the Advanced Trends in Mechanical and Aerospace Engineering*: *ATMA*-2019, Bangalore, India, 030016.
31. Saleem, H.; Edathil, A.; Ncube, T.; Pokhrel, J.; Khoori, S.; Abraham, A.; and Mittal V. (2016). Mechanical and thermal properties of thermoset-Graphene nanocomposites. *Macromolecular Materials and Engineering*, 301(3), 231-259.
32. Ligati, S.; Ohayon-Lavi, A.; Keyes, J.; Ziskind, G.; and Regev, O. (2020). Enhancing thermal conductivity in graphene-loaded paint: Effects of phase change, rheology and filler size. *International Journal of Thermal Sciences*, 153, 106381.
33. Asim, N.; Badiei, M.; Samsudin, N.A.; Mohammad, M.; Razali, H.; Soltani, S.; and Amin, N. (2022). Application of graphene-based materials in developing sustainable infrastructure: An overview. *Composites Part B*: *Engineering*, 245, 110188.
34. Das, S. (2017). *Graphene reinforced aluminum foam for automobile and aerospace*. Lambert Publishing.
35. An, Y.; Yang, S.; Zhao, E.; Wang, Z.; and Wu, H. (2018). Fabrication of aluminum foam reinforced by graphene nanoflakes. *Materials Letters*, 212, 4-7.
36. Wang, H.; Ma, C.; Zhang, W.; Cheng, H.-M.; and Zeng Y. (2019). Improved damping and high strength of graphene-coated nickel hybrid foams. *ACS Applied Materials & Interfaces*, 11(45), 42690-42696.
37. Antenucci, A.; Guarino, S.; Tagliaferri, V.; and Ucciardello, N. (2015). Electro-deposition of graphene on aluminium open cell metal foams. *Materials & Design*, 71, 78-84.
38. Dong, P.; Long, C.; Peng, Y.; Peng, X.; and Guo, F. (2019). Effect of coatings on thermal conductivity and tribological properties of aluminum foam/polyoxymethylene interpenetrating composites. *Journal of Materials Science*, 54(20), 13135-13146.
39. Sang, M.; Shin, J.; Kim, K.; and Yu, K.J. (2019). Electronic and thermal properties of graphene and recent advances in graphene based electronics applications. *Nanomaterials*, 9(3), 374.
40. Mohammed, T.W.; Rahmah, N.M.; and Jawad L.A. (2023). Thermal properties of nano-composites: A comparative study between epoxy/graphene and Epoxy/$CaCO_3$. *Journal of Engineering Science and Technology*, 18(1), 424-436.
41. Statnano (2023). Heat thermal insulation paint. Retrieved December 19, 2023, from https://product.statnano.com/product/11533/heat-thermal-insulation-paint.
42. Jeng, M. (1998). Can hot water freeze faster than cold water? Retrieved December 19, 2023, from https://math.ucr.edu/home/baez/physics/General/hot_water.html.
43. Chen, Z.; Lian, X.; Tan, J.; Xiao, H.; Ma, Q.; and Zhuang, Y. (2023). Study on heat-exchange efficiency and energy efficiency ratio of a deeply buried pipe

energy pile group considering seepage and circulating-medium flow rate. *Renewable Energy*, 216, 119020.

44. Zhang, L.; Mullen, D.; Lynn K.; and Zhao, Y. (2009). Heat transfer performance of porous copper fabricated by the lost carbonate sintering process. *Materials Research Society symposia proceedings*, 1188, 1188-LL04-07.
45. Holman, J.P. (2010). *Heat transfer*. The McGraw-Hill Companies.
46. Ahmad, M.I.; Yatim, Y.M.; and Masitah, A.R.S. (2015). Heat transfer and effectiveness analysis of a cross-flow heat exchanger for potential energy recovery applications in hot-humid climate. *Energy Research Journal*, 6(1), 7-14.
47. Pongiannan, S.; Ramalingam, V.; and Nagendran, L. (2019). Natural-convection heat transfer enhancement of aluminum heat sink using nano coating by electron beam method. *Thermal Science*, 23(5 Part B), 3129-3141.
48. Sabarish, R.; Hussain, J.H.; Kumar, S.K.P.; and Vignesh, S. (2015). Experimental investigation of heat transfer analysis on nano graphene coated extended surface. *International Journal of Innovative Research in Science, Engineering and Technology*, 4(3), 1-16.
49. Hasan, K.M.F.; Bai, S.; Chen, S.; Lin, K.; Ahmed, T.; Chen, J.; Pan, A.; Zhu, Y.; Lin, C.S.K.; and Tso, C.Y. (2024). Nanotechnology-empowered radiative cooling and warming textiles. *Cell Reports Physical Science*, 5(9), 102108.
50. Kline, S.J.; and McClintock, F.A. (1953). Describing uncertainties in single-sample experiments. *Mechanical Engineering*, 3-8.